Physics – Uspekhi **47** (12) 1239 – 1255 (2004)

METHODOLOGICAL NOTES PACS numbers: **01.50. – i**, **42.25. – p**, **42.65. – k**

Bi-frequency pendulum on a rotary platform: modeling various optical phenomena

B Ya Zeldovich, M J Soileau

DOI: 10.1070/PU2004v047n12ABEH001880

Contents

Abstract. The teaching of optical phenomena can be enhanced through the use of analogies to the motion of a bi-frequency pendulum. In this text we target demonstrations to four groups of students and scientists: younger schoolchildren to high school seniors; 7th graders to college juniors; college juniors to final-year graduate students in physics, optics and engineering; and college seniors to research scientists. The main difference between the groups is in the level of mathematics required to make the analogy to optical phenomena. Most of the physical ideas may be understood and appreciated even in junior high school and serve as a motivation for deeper study of mathematics and science.

B Ya Zeldovich, M J Soileau University of Central Florida, College of Optics and Photonics/CREOL,
4000 Central Florida Blvd, Orlando, FL 32816-2700, USA
Tel. (407) 823 68 31, (407) 823 55 38. Fax (407) 823 68 80
E-mail: boris@creol.ucf.edu, mj@mail.ucf.edu

Received 2 April 2004, revised 8 August 2004
Uspekhi Fizicheskikh Nauk **174** (12) 1337 – 1354 (2004)
Translated by B Ya Zeldovich, M J Soileau; edited by M V Chekhova

1. Introduction

Teaching various phenomena of optics and explaining their relationship to physics and engineering are noble and challenging tasks. Excellent university-level textbooks in the field of optics [1 – 6] coexist side-by-side with lay-level descriptions of fascinating optical phenomena in nature and in man-made devices [7 – 10]. Analogies with mechanical motion help students to better digest the ideas of both optics and mechanics.

A favorite mechanical demonstration is the propagation of transverse waves along a rope or a string kept at a certain tension; see, e.g., [6, p. 18]. Qualitative observation of the mechanical motion is accompanied by demonstrating the transverse nature of light by watching light pass through polarizing sunglasses; this is suitable even for kindergarten

children and is quite affordable for their parents or supervisors. In addition, with only a minor degree of complexity one can demonstrate the effect of polarization selectivity using a simple mechanical construct. At the Middle-School level one can perform quantitative measurements of the speed of mechanical wave propagation and its functional dependence on the tension strength.

This paper is devoted to the description of a particular mechanical device, the bi-frequency pendulum. This versatile device can be used to demonstrate motion and its relation to phenomena in optics to diverse levels of audiences: from younger schoolchildren to research scientists.

2. The device

The main object of this paper's study is a pendulum that can swing in two directions, denoted below as x and y, with gravity serving as the restoring force. The x- and y- directions of mechanical motion serve mostly as substitutes for the polarization directions of an optical wave. Other analogies will be discussed below as well.

A pendulum hanging from a single pivot point yields the same periods of small oscillations in both directions, x and y, and, as a consequence, the same period for any other superpositions of the above motions. The demonstrations described below are based on the fact that the design shown in Figure 1 is comprised of slightly different lengths to the effective pivot point, $L_x < L_y$, for small oscillations in the x- and y-directions. A doorframe with two nails in it (Fig. 1a) is quite suitable for this demonstration, if rotation of the frame is not required. The length of the string may be about 1 to 2 m, yielding a period of oscillation $T = 2\pi\sqrt{L/g}$, about 2 to 3 s, which is convenient for measurements. A small n-percent change in the effective length leads to an $n/2$-percent change in the period. Therefore, the length difference $L_y - L_x$, about 0.1 m for the 1-meter pendulum, yields the frequency difference $f_x - f_y = (1/T_x) - (1/T_y)$, about 0.025 Hz. Thus, the period of beats T_b is about 40 s, which gives plenty of time to watch the gradual changes in the 'polarization state', see below. Some familiar household devices can be easily converted to effective and inexpensive teaching tools. A builder's plumb bob offers a well-centered way to attach the string. A rather heavy bob, 140 to 230 g (5 to 8 oz.) may be used to diminish the damping. A tabletop 'Lazy Susan' makes a good platform; it has a ball bearing providing rotation. Iron plumbing pipes (1.27 cm or $1/2''$ in diameter) with angular or T-couplers may be used to make a frame, which is affordable and is made of parts available at any hardware store. It can be attached to the platform by wide-diameter iron flanges (for rigidity). Pipes about 1 meter in height can be made using two 0.5 m pipes tightly connected together, making them easier to transport. Some models were actually built with a smaller mass and with L about 0.3 m, based on the 'Health' disc of old Soviet production. These models are easier to transport; however, the damping may be uncomfortably large.

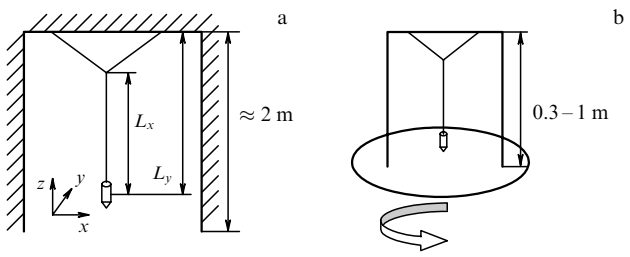

Figure 1. Bi-frequency pendulum. (a) A rather heavy plumb bob, 140 to 230 g (5 to 8 oz.) was used with the aim of diminishing the damping. A door frame with two nails in the top bar served as an excellent support. (b) The 'Lazy Susan' food serving device provided a reasonably good platform with a ball bearing for its rotation. We used mostly $L_x \approx L_y \approx 1$ m, $L_x - L_y \approx 0.1$ m, so that $T_0 \approx 2$ s, $T_{beats} \approx 40$ s. Some models were built with smaller mass and with L about 0.3 m, but then the damping could be uncomfortably large.

The pendulum can be easily excited by using small fans (from microchip coolers) to blow air in a prescribed direction with precise frequency. The fans used were fed by a DC power supply, 12 to 26 V, and the periodicity was achieved by controlling the current by a MOSFET; in particular, Radio Shack's IFR-510 served quite well. The low-current signal, which was controlling the current supplied to the fans, had the amplitude of several volts applied between MOSFET's gate and source. The main current was flowing from drain to source and was thus controlled by the signal. A frequency-tunable signal generator produced the control signal. We successfully explored the possibility of generating a controlling signal from a computer via its standard (and hence, at no extra cost) sound card, and later used that approach exclusively. Particular implementation used specially designed freeware 'Square pulse' [11], which produced rectangular AC pulses of about 1.5 V in amplitude at the output of the sound card. Rectifying those AC pulses with a voltage doubling scheme and using DC bias from two AAA batteries, we could get stable control of periodic air flow. Several small fans have a faster response to time-varying voltage than does one large fan. This is important if the frequency in question is higher than or about 0.5 Hz, as above.

The following sections of this paper are devoted to the description of various demonstrations with the pendulum and their relations to optical phenomena.

3. First level: from younger schoolchildren to High-School seniors

3.1 The superposition principle as derived from isochronism

A mono-pivotal pendulum on a stationary frame is simple and quite suitable for a variety of important demonstrations. One should measure the period of motion for a 1-cm deflection (zero-to-maximum) of, e.g., a 1-meter long pendulum. The period is about 2 s; the exact value depends on the details, for instance, how the bob is attached to the string. Measuring the time of about 10 or 20 full oscillations yields good accuracy if the starting and ending points of the count are at the same phase of motion and the count is started by an exclamation 'zero' after one or two initial oscillations. A larger number of swings may lead to a noticeable decrease in the amplitude, and thus contradicts the purpose of the experiment. The next step is to measure the period for a 3-cm deflection. The period and the character of motion, as depicted by the approximate graph $x(t)$, turn out to be the same as for the 1-cm deflection (Fig. 2a). Then the same is done with 2-cm and 4-cm amplitudes, obtaining the same results (Fig. 2b). A plausible conclusion can be made by the teacher: one can add (1 cm +3 cm = 4 cm), subtract

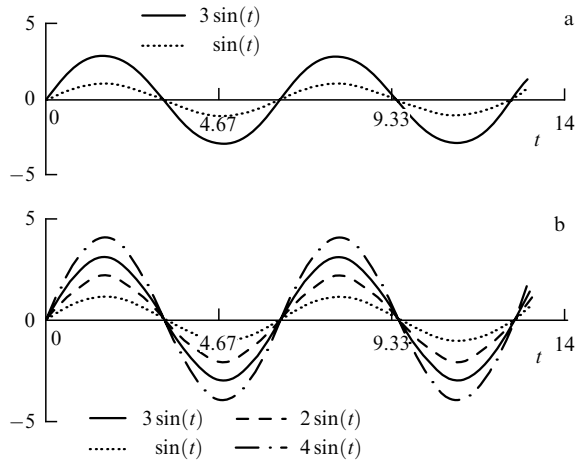

Figure 2. Illustration of the superposition principle. (a) Oscillations with the amplitudes 1 cm and 3 cm have the same period and, plausibly, the graphs of the motion are different by the vertical scale (factor 3) only. (b) One can add (1 cm +3 cm = 4 cm), subtract (3 cm −1 cm = 2 cm), and multiply by a number (1 cm ×3 = 3 cm) various motion functions $x(t)$, and each time obtain valid motion functions.

(3 cm −1 cm = 2 cm), and multiply by a number (1 cm $\times 3_{\text{number}}$ = 3 cm) various motion functions $x(t)$ and each time obtain valid motion functions. The teacher should tell the audience that the 'superposition principle' is thus established.

3.2 Resonance

A student should be asked to deflect the pendulum by blowing in a constant way (DC, in electronic terminology). A relatively heavy plumb bob, 150 to 250 g, can be deflected in this way at a very small angle only. The next step is to ask the students if they can invent a way to get a larger deflection. Quite soon they discover the idea of blowing 'in resonance'. Two students excite the oscillations especially effectively when they blow from opposite sides of the pendulum periodically one after another.

3.3 Polarization

Using a single-pivot pendulum, the teacher should suggest to the students that they generalize the Superposition Principle to an area that has not yet been covered by experiment: superposition of x- and y-oscillations, say, with equal strengths. Adding $x(t)$ and $y(t)$ 'in-phase', one gets '+45°-polarization', using optical terminology. Adding $x(t)$ and $y(t)$ with 180° phase shift, one gets '−45°-polarization'. With a time delay $+T/4$ or $-T/4$ between the original $x(t)$ and $y(t)$, one gets 'right circular' and 'left circular' polarizations. Elliptical polarizations of all types constitute a natural continuation of these observations.

Playing with polarizers is real fun, and should definitely accompany mechanical experiments with the pendulum and the waves on a rope or a string. Class-wide optical demonstrations are more cost-effective if a large sheet of polarizing film is bought (e.g., from *Edmund Scientific*) and then cut into small pieces. Demonstrations can also be facilitated by commercial polarizing sunglasses, about $10 apiece. A combination of polarizing glasses and polarizing filters that can hang on one's regular glasses is especially convenient. Glasses offer the advantage of sitting firmly on one's face and do not require an extra hand to hold them, while filters can be easily manipulated by one hand, leaving the other hand for further experiments. The blue color of the sky and specular reflections from dielectric surfaces (not necessarily transparent ones) are natural and important sources of polarized light (the Brewster effect). These must be compared to metallic reflections, diffusive reflections, and white clouds, which generate non-polarized light.

3.4 Dependence of the oscillation period T on the pendulum's length L

Quite traditional (albeit important) experiments should be done to measure the dependence of the oscillation period T on the pendulum's length L. The qualitative character of this dependence, that T grows as L grows, is easily observed and understood even at the kindergarten level. An exact graph of the square of the period T^2 versus the length L should give straight line; this allows visualizing experimental errors.

After that short introductory study of and playing with the mono-pivotal pendulum, we now return to the bi-frequency pendulum.

3.5 Beats of the bi-frequency pendulum

The basic experiment is started by launching '+45°-polarized' motion. The relative phase delay between x- and y-oscillations gradually grows. When it reaches $\pi/2$, one observes 'circularly polarized' motion. The evolution of motion up to this moment is analogous to the action of a quarter-wave plate upon a monochromatic light beam. At the moment when the phase delay reaches π, one observes '−45°-polarization'; this is equivalent to the action of a half-wave plate in optics. Then the process goes through 'elliptically polarized' stages to the circular motion of opposite sign, $3\pi/2$ phase shift. The complete period of beats T_b corresponds to the return to the original '+45°-polarized' motion. Good observation conditions are achieved if the period of beats T_b is much longer (30 to 50 times) than the basic period T of the pendulum's oscillations. Then one can appreciate the 'instantaneous view' of the polarization state, as if it consisted of the discrete stages depicted in Fig. 3.

3.6 Colors of stressed plastic positioned between crossed polarizers

This demonstration requires a piece of plastic in which strong anisotropy was induced in the thermo-manufacturing process, or is induced by applying a bending force to the piece. An audiocassette case or a transparent plastic ruler usually have

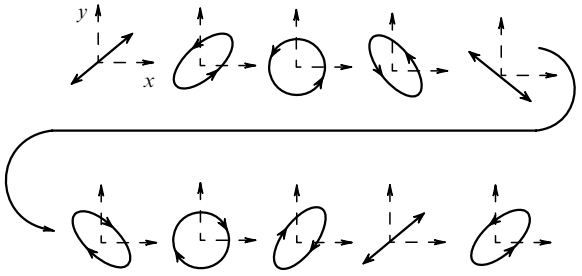

Figure 3. Sequence of the motion patterns of a bi-frequency pendulum. The 'instantaneous view' of the polarization state, as if it consists of discrete stages, is depicted in the figure. We start with the value $x(t=0) = y(t=0) = a$, $\mathrm{d}x/\mathrm{d}t|_0 = \mathrm{d}y/\mathrm{d}t|_0 = 0$ (upper left entry, +45°-polarization), i.e., with zero phase difference between x and y. Each subsequent pattern corresponds to a $(\pi/4)$-increment of the phase difference, so that in the last entry (lower right), this difference is equal to $2\pi + \pi/4$.

the needed anisotropy. One should place this piece between crossed polarizers. The best way to watch the resulting color patterns (usually very beautiful) is to look at a spatially extended source of white light, e.g., a white ceiling or a fluorescent lamp. One should take the time to watch the patterns under independent changes of orientation of both the plastic element and polarizer. Use of the blue scattered light of the sky as the source of reasonably well-polarized light refreshes the knowledge of the properties of Rayleigh scattering; in this case only one analyzer is sufficient. Another well-accessible source of polarized light is a beam of specular reflection from a dielectric (glass, a floor tile, etc.).

The teacher may discuss the time delay of one polarization component in comparison with the other one. The delay is almost the same for all visible colors. However, the same time delay constitutes different fractions of the optical cycle for different wavelengths and that is the explanation for the nice color patterns.

4. Second level: from 9th grade of High School to 4th year of undergraduate program

4.1 Measurement and calculation of the beat period T_b

First, one should separately measure the periods for x- and y-oscillations with the best possible accuracy. Using a larger number of periods, almost down to a complete stop, is permitted here, since the isochronism of small oscillations has already been established. Important reminder: make sure to start all counts with 'zero' instead of 'one'. The next step is to measure the complete period of beats T_b, the time when the polarization comes back to its original state.

Here is the reasoning, which even the least math-oriented students will probably understand. One complete extra period of x-oscillations is covered during the time T_b in comparison with the y-oscillations:

$$T_b = NT_y = (N+1)T_x\,.$$

Hence,

$$N(T_y - T_x) = T_x\,.$$

Therefore,

$$T_b = \frac{T_x T_y}{T_y - T_x}\,.$$

This actually means that the beat frequency

$$f_b = \frac{1}{T_b} = f_x - f_y\,.$$

It is important to compare the measured period of beats with the value from the above calculations. It is also worth discussing the formula

$$T_b \approx \frac{T_0^2}{T_y - T_x}\,.$$

Any formula claiming better accuracy is senseless, since T_b is not well defined experimentally for incommensurate T_x and T_y [1].

[1] According to legends about L D Landau, he could forgive somebody for making an honest mistake in a scientific work, but 'overestimation of accuracy' (i.e., not taking into account all the terms of the given order of perturbation theory) was considered by him to be a deadly sin.

One should also teach students how good accuracy may be achieved. Individual effective lengths for x- and y-oscillations cannot be measured very accurately, since the position of the bob's center of gravity, first, cannot be well observed, and, second, is not directly connected with the oscillation period (e.g., one must calculate the moment of inertia). To the contrary, the small difference ΔL between L_y and L_x can and should be measured with good accuracy.

4.2 Lissajous figures, the Foucault pendulum, and uniaxial crystals

Senior participants in the demonstrations declare quite frequently that this is a *Foucault pendulum* and that the motion observed may be classified as *Lissajous figures*. Teacher, beware: none of the above statements is true; see comments in Appendix 8.1. Besides that, Appendix 8.2 contains comments on depicting the properties of uniaxial crystals with the use of a bi-frequency pendulum. However, the analogy is purely visual.

We present below in Sections 4.3 and 4.4 the description of two mechanical experiments aimed at understanding how a Liquid Crystal Display works.

4.3 Preservation of polarization direction under fast turning of the platform

One should start with a pure-mode motion, e.g., with pure y-motion (lower-frequency mode). Fast turning of the platform by 90° keeps the polarization unchanged in 'absolute space' and hence the motion is switched into high-frequency mode: into x-mode, from the point of view of the platform. The same situation occurs with the $x \to y$ transformation under fast turning of the platform by 90°. Such behavior is described in scientific literature as 'anti-adiabatic' motion. Actually, the preservation of polarization in absolute space also holds for fast turning by any angle, but then the resultant motion will demonstrate typical beats, shown previously in Fig. 3.

4.4 Adiabatic following

Start the rotation of the platform gradually: by much less than 90° for a time equal to the period of beats. Then one sees a surprising result. Namely, the original 'linear polarization' stays linear and seems to *follow adiabatically* the instantaneous orientation of the frame. (By the way, here one should reject any recollections about the use of the word 'adiabatically' in molecular physics.) The same result is equally valid with the other linearly polarized eigenmode. The important thing is the smoothness and slowness of switching the rotation 'on' and 'off'. During the rotation, in-between 'on' and 'off', the polarization becomes slightly elliptical, but at the end it will be restored to the original linear type of polarization, to the original eigenmode.

There are additional experiments for preparing the audience for the explanation of the adiabatic following regime. One should start a linearly polarized (e.g., low-frequency) y-eigenmode, and then quickly turn the platform by a small angle, e.g., by 15°. The performer should direct the audience's attention to excitation of the other mode (x-mode). This excitation, even if small, reveals itself clearly by the subsequent rise in elliptical motion, as in Fig. 3. Launch the pure y-eigenmode again, at this new position of the platform, and again quickly turn the platform in the same direction, at the same small angle, and with the same result.

Here is the explanation of adiabatic following that is both scientifically correct and may be understood at the lowest

level of mathematics comprehension. Under slow rotation, the device continuously 'tries' to excite the 'wrong' mode (see the above preparatory experiments). However, it tries to excite the high-frequency mode using for that purpose the low-frequency excitation force from the actual oscillations present. But we have seen in the experiment in Section 3.2 that excitation out of resonance is not effective. Therefore, the 'wrong' mode is not excited to any considerable level. This is not an easy point, and time should be allocated to digest it. Actually, there is a one-to-one correspondence between this seemingly primitive explanation and the Slowly Varying Envelope Approximation (SVEA) of the Maxwell equations in a twisted anisotropic medium (shortened equations in Russian scientific terminology; one of the authors, B Ya Z, learned these from his informal teachers, R V Khokhlov and S A Akhmanov). Therefore, this explanation is worth learning; it introduces the general notion of adiabatic following.

An additional pendulum demonstration is related to the explanation of how Liquid Crystal Displays work. Pulling two supporting strings strongly in opposite directions, one can effectively transform our pendulum into a mono-pivotal device. Symmetry implies that this new pivot point will be on the platform's axis. Then, no rotation, be it slow or fast, can influence the pendulum's oscillations in absolute space. Interpretation of this in the platform's frame is that now all eigenmodes are degenerate, i.e., have the same frequencies and, hence, excitation of the 'wrong' mode (by the Coriolis force, by the way) is always in resonance.

Appendix 8.3 contains an everyday analogy for explaining the qualitative difference between the two regimes, adiabatic and non-adiabatic. However, that example does not have an underlying similarity of equations.

4.5 How Liquid Crystal Displays (LCDs) work

Switching from the regime of adiabatic following to the regime of plane preservation for a pendulum in absolute space is analogous to the principle of operation of LCD-displays in watches, calculators, and a multitude of other devices. Numerous excellent descriptions of the mechanism of LCDs exist in the literature; we can recommend, for example, monographs [12, 13]. One should first demonstrate the presence of the input polarizer inside the display by watching it through another polarizer, e.g., sunglasses. Most people are actually surprised by this observation. Next, one should give a short description of the Nematic Liquid Crystal (NLC), whose anisotropic molecules produce a noticeable difference in the speed of light for two mutually orthogonal linear polarizations. A discussion of the softness of the orientation of the NLC and polishing technology to fix the orientation at the cell walls explains the design of the Twisted Nematic LCD (TNLCD). This can be followed by a description of the second polarizer (working actually as an analyzer) oriented at 90° to the input polarizer. Then matted aluminum foil should be mentioned, which reflects light in a diffuse manner but preserves its polarization. Finally one should describe the role of miniature flat electrodes, which are electrically conductive but surprisingly transparent.

The TNLCD works in the following manner. When no voltage is applied to the electrodes, adiabatic following leads to a 90° rotation of polarization by the 90°-twisted nematic, and a crossed polarizer/analyzer pair transmits light back and forth — this is the 'white' background of the display (Fig. 4a). When the voltage is applied to a particular group of

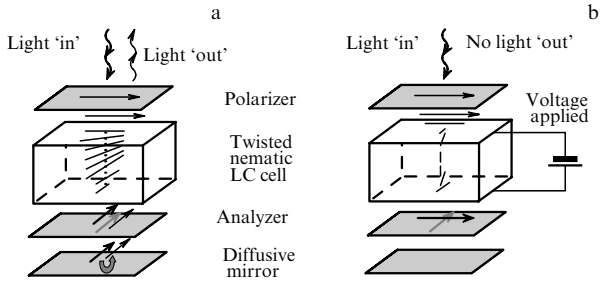

Figure 4. How a Liquid Crystal Display (LCD) works. (a) An input polarizer polarizes incident light. During propagation the electric vector of light follows adiabatically the orientation of the twisted nematic. Therefore, light is transmitted by the crossed analyzer, diffusely reflected and transmitted back. This is the white background of a display. (b) Application of voltage to the cell's transparent electrodes yields vertical isotropic orientation of the nematic. As a result, propagation does not change the electric vector of light, and the crossed analyzer absorbs the light. This is the blackened element of the display.

electrodes, the electric field orients the NLC vertically, just as pulling two ends of the string makes the pendulum isotropic. Then, the polarization stays intact in absolute space and the crossed analyzer blocks the transmission of light — this is the dark part of a digit or letter (Fig. 4b). Actually, AC voltage is commonly used to suppress the electrolysis processes.

Two limiting cases will help in digesting and remembering this information. If the battery is dead or removed from the device altogether, the adiabatic following is in place all over the screen and the entire surface is 'white'. If the liquid crystalline material leaks out of a part of the cell, then the corresponding part of the display is dark due to the action of crossed polarizers, independently of the presence or absence of the battery.

4.6 Notions of the carrier frequency and the modulation envelope

Launching +45°-polarization means excitation of both modes, x and y, with equal amplitudes. It is easy to arrange an observer's position by the pendulum in such a way that they see +45°-projection only. Then, the signal $S_{45}(t)$ is equal to

$$S_{45}(t) = 0.5A_0\left[\cos(2\pi t f_x) + \cos(2\pi t f_y)\right] \equiv A_0 \cos\left[\frac{2\pi t(f_x - f_y)}{2}\right] \cos\left[\frac{2\pi t(f_x + f_y)}{2}\right]. \quad (1)$$

A simple trigonometric identity was used to get the second expression. It contains the product of two factors. The first is the envelope that describes beats. The second is the carrier-frequency cosine function. The period of beats, as we know, is

$$T_b = \frac{1}{f_x - f_y}.$$

Meanwhile, the envelope reproduces itself after two complete beat cycles only, $2T_b$ (see the graph in Fig. 5). It is only the square of the envelope, or intensity, which has the standard beat period T_b. The human eye does not recognize the change in the sign of the envelope, since the phase of the carrier is not captured by human perception. To elucidate this change of sign, one can attach a second pendulum to the same frame (see

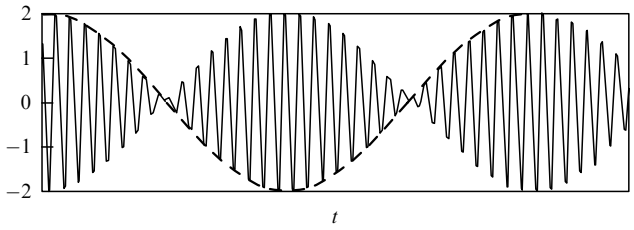

Figure 5. Beats as observed in the projection to the +45° axis. Carrier-frequency oscillations are multiplied by the amplitude envelope. The sign of the envelope is restored after two (2!) complete periods of beats of the intensity.

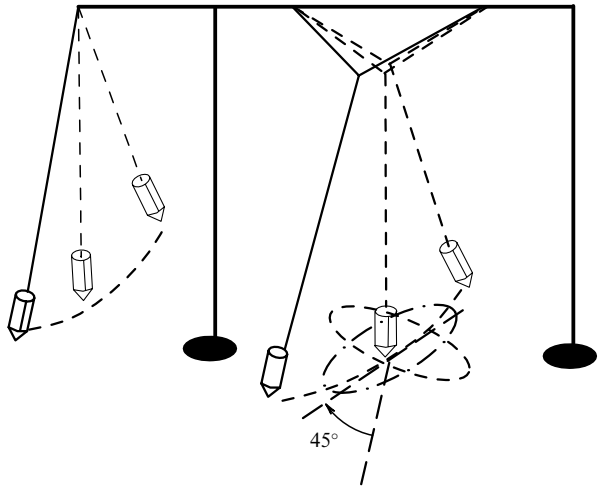

Figure 6. Setup demonstrating the sign of the envelope for the interference case. The auxiliary pendulum is tuned to the 'carrier' frequency, i.e., the frequency equal to the arithmetic average $(f_x + f_y)/2$ of the frequencies of x- and y-oscillations.

Fig. 6) and spend some time adjusting its frequency to the carrier, i.e., to the arithmetic average $(f_x + f_y)/2$. Then one launches both the bi-frequency pendulum and the reference one in the same +45°-direction and with the same initial phase. Watching the +45°-projection only, one observes a visually surprising result described by unsurprising formula (1): the envelope of beats changes its sign after one cycle of beats; the sign is restored after two complete beat cycles only!

Two phenomena (and maybe more) in physics produce this change of sign after one cycle and complete restoration after two cycles; they are discussed in Sections 6.8 and 6.9.

5. Third level: from 3rd-year undergraduate to 5th-year graduate students

5.1 Resonance curve and phase shift under detuning

One should write Newton's Second Law equation for a frictionless harmonic oscillator, which has an eigenfrequency f_0 and is subjected to the action of monochromatic external force $A\cos(2\pi ft)$:

$$m\left[\frac{\mathrm{d}^2x}{\mathrm{d}t^2} + (2\pi f_0)^2 x(t)\right] = A\cos(2\pi ft)\,. \tag{2}$$

Generally, the frequency f of this external force is not equal to the eigenfrequency f_0 of the oscillator. The steady-

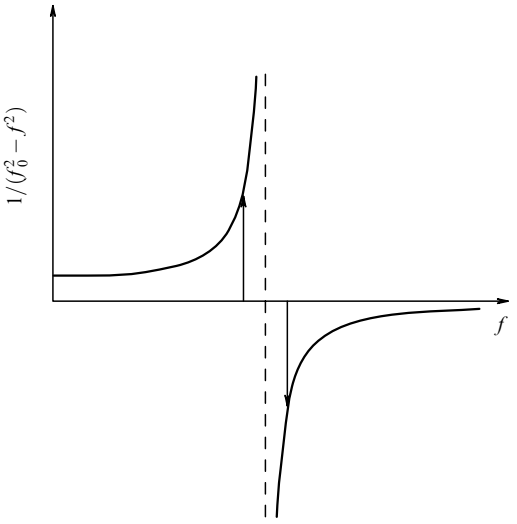

Figure 7. Standard resonance curve: response of a linear harmonic oscillator versus frequency f of the applied force. The phase change by 180° at the passage of the resonance should be emphasized.

state solution of this equation is reached if one considers the presence of an infinitesimally small friction; however, the solution itself is finite even in the approximation of zero damping:

$$x(t) = \frac{A}{(2\pi)^2 m}\,\frac{\cos(2\pi ft)}{f_0^2 - f^2}\,. \tag{3}$$

The graph of this simple but important function, $1/(f_0^2 - f^2)$, is shown in Fig. 7. Quantitative measurement of this curve for the pendulum is rather difficult: one should change the frequency f of the applied force while keeping its amplitude A constant, the latter requirement providing the main obstacle. However, one can demonstrate the striking character of the curve. The response is 'in phase' with the force when the external force has the frequency f below resonance, $f < f_0$, and the response is 'counter-phase', i.e., with a phase shift 180° to the force, when the external force is above resonance, $f > f_0$. In the vicinity of the resonance one may use the approximation

$$\frac{1}{f_0^2 - f^2} = \frac{1}{(f_0 - f)(f_0 + f)} \approx \frac{1}{2f_0(f_0 - f)}\,. \tag{4}$$

Then, equal small detuning values $|f_0 - f|$ above and below resonance produce equal responses, but one is 180° phase shifted with respect to the other (see Fig. 7).

It is here that the setup with small fans controlled from a signal-generator or from a computer's sound card is used for the first time. The moments of the positive maximums of the force are clearly recognized if one listens attentively to the buzz sound generated by the fans.

By the way, the 90° value of the phase shift at exact resonance, as well as the finite value of the response amplitude at exact resonance, requires taking friction into account. This 90° phase shift at exact resonance is also easily observable with the use of the excitation device described above.

Certain ingenuity is required to demonstrate equal moduli and 180°-shifted phases of the responses at the small detuning values above and below the resonance, Eqn (4). Here, the bi-

frequency pendulum may be used. If monochromatic force is applied in the $+45^\circ$ direction, then the moduli and the phases of the x- and y-components of the force are the same. Meanwhile, if at the same time the frequency f of this force exactly equals the arithmetic average of two eigenfrequencies, $f = (f_x + f_y)/2$, then the moduli of x- and y-responses are the same, but the phases are shifted by 180°. As a result, steady-state oscillations are oriented at -45°. Such a motion of the pendulum looks extremely counter-intuitive and hence gives a lot of food for thought!

The following optical and electromagnetic phenomena may be discussed after the above demonstrations. The refractive index of glass and of most other materials transparent in the visible range is due to strong resonance transitions in the UV range. That is why the response of the medium is *positive*, and the relative dielectric constant $\varepsilon/\varepsilon_0$, along with the refractive index n, are greater than 1.

On the contrary, plasma (e.g., free electrons in the ionosphere) has zero eigenfrequency of the equivalent oscillators, since the restoring force is zero for free electrons. Therefore, the response of the medium is *negative*. The dielectric constant $\varepsilon/\varepsilon_0$ and the refractive index n are below their vacuum value 1. Polarizability is proportional to $\varepsilon/\varepsilon_0 - 1$ and it is *negative* for almost any material if the wavelength of incident radiation is in the X-ray spectral range.

5.2 Violations of the superposition principle and nonlinear self-precession of an ellipse

Being extremely important, the superposition principle still looks rather bland until an example of its violation is shown. Take the circularly polarized motion of a 1-meter long pendulum with a deflection of about 0.5 m, i.e., $\varphi = 30^\circ$ from the vertical axis. An attempt to superimpose two such motions, i.e., to get the 60°-motion, leads to a considerably faster rotation: $T_\varphi = T_0(\cos\varphi)^{1/2}$, so that $T_{30} = 0.931 \cdot T_0$, while $T_{60} = 0.707 \cdot T_0$. One can easily obtain as high a frequency as safety allows by making the angle close to 90°. A shorter string helps for this demonstration.

Actually, violation of the superposition principle for linearly polarized motion can be deduced 'theoretically' from the approximate representation of linear motion as a superposition of two circular motions, right and left, with equal amplitudes. Nevertheless, a direct demonstration of nonlinearity is preferable.

For a visible demonstration of nonlinearity one can start with a simple (mono-pivotal) isotropic pendulum. Linearly polarized motion stays linear at any amplitude. Similarly, circularly polarized motion stays circular at any amplitude. A qualitative difference is observed for elliptical motion of finite amplitude. The size of the ellipse is preserved; it is equivalent to the energy conservation. The ratio of the small axis of the ellipse to the large one stays constant; this is due to the conservation of angular momentum. However, the orientation of the ellipse shows gradual precession and this is the manifestation of nonlinearity. Indeed, this slow precession of elliptical motion can not be described as a superposition of two linearly polarized motions of fixed orthogonal directions — the description that worked perfectly for infinitesimally small amplitudes. The precession is actually in the same direction in which the bob revolves along the ellipse but it takes many oscillations to get a noticeable precession angle, if the amplitude of motion is much smaller than 1 radian.

The nonlinear-optical analog of this precession is the phenomenon of the self-rotation of polarization ellipse, observed in 1964 by Maker, Terhune, and Savage [14]. The rate of self-rotation (radians per meter of propagation) was proportional to the expression that was similar to the result described by equations (28)–(30) in Section 6.11 of the present paper.

5.3 Rotary Doppler effect

In this demonstration the rotary platform is used but the pendulum should be mono-pivotal. Begin by launching a linearly polarized motion, and then rotate the platform with constant angular velocity $\mathbf{\Omega} = \mathbf{e}_z\Omega$. Since a single pivot is situated exactly on the axis of rotation, polarization stays intact in 'absolute space'. This means that the plane of linearly polarized motion changes its orientation with respect to the platform. Hence, it is not an eigenmode from the point of view of the platform's coordinate frame. However, circular motions are equally circular in any rotating or non-rotating frame. Thus, one can say that the circular motions of a mono-pivotal pendulum constitute eigenmodes even in a rotating frame. One important observation should be made during this demonstration. If the pendulum rotates in 'absolute space' in the same direction as the platform (co-rotation), then an observer at the platform perceives a smaller angular frequency of rotation: $\omega(\textit{co-rotation}) = \omega_0 - \Omega$, where $\omega_0 = \sqrt{g/L}$. In fact, counter-rotation of the platform and pendulum is perceived as circular motion with higher angular frequency: $\omega(\textit{counter-rotation}) = \omega_0 + \Omega$. This is a reasonably good analog of the Doppler effect, as applied to rotary motion. A dynamic description of this essentially kinematic phenomenon from the point of view of an observer at the rotating platform is rather complicated. Namely, one should add the gravity-induced restoring force of the string to centrifugal and Coriolis inertia forces, and then equalize this sum to mass times centripetal acceleration.

5.4 Magneto-optical rotation of polarization

The notion of rotary Doppler effect has an important application in the optics of a medium placed in external magnetic field $\mathbf{B}$. Consider first the small angular velocity of the rotating frame, $\Omega \ll \omega_0$. One may then neglect centrifugal force as a quantity $\propto \Omega^2$, and take into account the linear part of the inertia force only: the Coriolis force $\mathbf{F}_\mathrm{C} = 2m[\mathbf{v} \times \mathbf{\Omega}]$. One may choose the value and direction of Ω in such a way that this Coriolis force will exactly compensate the Lorentz force $\mathbf{F}_\mathrm{L} = q[\mathbf{v} \times \mathbf{B}]$, with which the externally applied magnetic field $\mathbf{B}$ influences the motion of electrons. Here, m and $q = -|q|$ are the mass and charge of an electron, respectively. This statement constitutes Larmor's famous theorem, and the corresponding angular velocity vector $\mathbf{\Omega}_\mathrm{Larmor}$ characterizes Larmor's precession of electrons in a weak (no Ω^2-terms) magnetic field $\mathbf{B}$:

$$\mathbf{\Omega}_\mathrm{Larmor} = -\frac{q\mathbf{B}}{2m}\,. \tag{5}$$

Henry Becquerel used the idea of Larmor's precession to estimate (calculate) the strength of Faraday's effect of the magnetically induced rotation of polarization. Consider an electromagnetic wave, which has angular frequency $\omega_0 \equiv 2\pi c/\lambda_0$ in the laboratory frame and propagates along an externally applied magnetic field $\mathbf{B}$; here, λ_0 is the wavelength of light in a vacuum. If the wave has right circular

polarization, the medium in the Larmor-rotating frame 'perceives' this wave at the Doppler-shifted frequency $\omega_R = \omega_0 + \Omega_{Larmor}$. Similarly, the left circularly polarized wave is 'perceived' by the medium in a rotating frame as if there were an opposite rotary Doppler shift: $\omega_L = \omega_0 - \Omega_{Larmor}$. Since Lorentz and Coriolis forces compensate each other, one may assume that effective refractive indexes for those two waves, n_R and n_L, 'know' nothing about any of the forces, $\mathbf{F}_C$ and $\mathbf{F}_L$. Therefore, one can use unperturbed refractive index n, but at the frequencies shifted due to the rotary Doppler effect:

$$n_R = n(\omega_0 + \Omega_{Larmor}), \qquad n_L = n(\omega_0 - \Omega_{Larmor}).$$

The linearized approximation yields

$$n_{R,L} = n(\omega_0 \pm \Omega_{Larmor}) \approx n(\omega_0) \pm \frac{dn}{d\omega}\,\Omega_{Larmor} \equiv n(\lambda_0) \pm \pi c\,\frac{dn}{d\lambda_0}\,\frac{qB}{m\lambda_0^2}. \quad (6)$$

The rate of Faraday's rotation of polarization, in radians per meter of propagation, is thus

$$\frac{d\varphi}{dz} = \frac{\pi(n_R - n_L)}{\lambda_0} = \frac{\Omega_{Larmor}}{c}\,\omega_0\,\frac{dn}{d\omega_0} = -\frac{\Omega_{Larmor}}{c}\,\lambda_0\,\frac{dn}{d\lambda_0} = -qB\lambda_0\,\frac{dn}{d\lambda_0}\,\frac{1}{2m_e c}. \quad (7)$$

This is Becquerel's approximate formula, connecting the Faraday rotation constant (the so-called Verdet constant) to the dispersion $\lambda_0\,dn/d\lambda_0$ of the material. The accuracy of this formula, at least outside the very vicinity of resonance, is surprisingly good: usually 20% or better for the majority of transparent materials. It means that the approximation of mutually non-interacting isotropic atoms (to which the Larmor theorem is really applicable) describes the Faraday effect reasonably well. This correlates with the well-regarded law of chemists: the refractivity $(n-1)$ of a medium is approximately the sum of refractivities of the constituting *atoms*.

Here is an easy way to remember the sign of the Verdet constant in Eqn (7). Magnetic field $\mathbf{B} = B\mathbf{e}_z$ may be created by the flow of electrons in a wire spooled as a solenoid. Larmor's precession of electrons in the transparent material inside the solenoid was built up when the magnetic field was gradually 'switched on'. By Lenz's rule, the sign of this precession is such that there is at least partial compensation of the increase in the magnetic flux through the solenoid. This means that the precession is *opposite* to the circular flow of electrons in the wires and, hence, *coincides* with the direction of electric current in the wires. Polarization of light is partially 'dragged' by the precessing electrons, and that prescribes the sign of Faraday's rotation by the external magnetic field. It is also instructive to mention that the Faraday effect must have an opposite sign for antimatter, as shown by the odd power of charge q in Eqn (7).

5.5 Parametric resonance

This topic is often raised during the demonstrations. Indeed, suppose that one pulls the string (and thus changes the length of the pendulum) to a periodicity two times shorter than the period of linearized oscillations. If friction and detuning are small enough or if the amplitude of length modulation is large enough, then parametric instability develops. Unfortunately, this particular demonstration with a pendulum has at least two drawbacks. First, to achieve small damping, one should use a sufficiently heavy bob. Under this condition, it is not easy to pull the string with a large enough amplitude and with very precise periodicity. Second, the most interesting application of parametric generators in optics deals with the possibility of generating light of a tunable wavelength, $1/\lambda(\text{pump}) = 1/\lambda_1 + 1/\lambda_2$, i.e., $f(\text{pump}) = f_1 + f_2$. The authors of the present study do not know how one can easily demonstrate tunable nondegenerate parametric oscillation or at least nondegenerate parametric amplification.

6. Fourth level: from second-year graduate students to research scientists

6.1 Device for modeling electromagnetically induced transparency (EIT) and the mathematics of damped coupled oscillators

Here is the mechanical device that was used for modeling electromagnetically induced transparency (EIT) — one of the most interesting phenomena of modern nonlinear optics. This device is a modification of the original bi-frequency pendulum, and no rotary platform is needed. The pendulum depicted in Fig. 8 has two slightly different effective lengths for two orthogonal oscillations, so that *if one ignores damping* (friction), one gets x- and y-axes as eigen-directions for the undamped modes, which have slightly different frequencies, $f_y < f_x$.

The mechanical design is based on the use of screws with sharpened ends that are attached to aluminum planks at an adjustable height. A vertical rod was attached to the lower plank in such a way that the rod could not rotate around the vertical axis, and a thin rigid sheet could be attached to the pendulum, playing the role of a 'sail'. The sail's purpose is to provide strong aerodynamic friction, i.e., damping with respect to the motion *perpendicular* to the sail's plane. Figure 8 shows an alternative variant of the design of a bi-frequency pendulum with a 'sail'; this design uses miniature ball-bearings.

Meanwhile, the friction with respect to the motion *in the direction* of the sail's plane is assumed to be very small. The particular choice of the sail's orientation was such that the motion in the $+45°$-direction was strongly dampened, while the $-45°$ motion was supposed to induce almost no loss of mechanical energy. If one ignores the x/y frequency splitting, then the $+45°$ and $-45°$ directions correspond to the eigenvectors of the damping operator.

One may say then that x and y motions are coupled via anisotropic ($+45°$ versus $-45°$) friction. At the same time, one may say that $+45°$ and $-45°$ motions are coupled via an anisotropic (x versus y) restoring force. To display the properties of our particular system more clearly, a general approach to the theory of coupled damped anisotropic harmonic oscillators is reviewed below.

Essential information about a general system is reduced to three positive-definite quadratic forms: the mass matrix M_{ik}, the elasticity matrix E_{ik}, and the damping matrix R_{ik}. These matrices define, respectively: kinetic energy

$$0.5M_{ik}\,\frac{dq_i}{dt}\,\frac{dq_k}{dt},$$

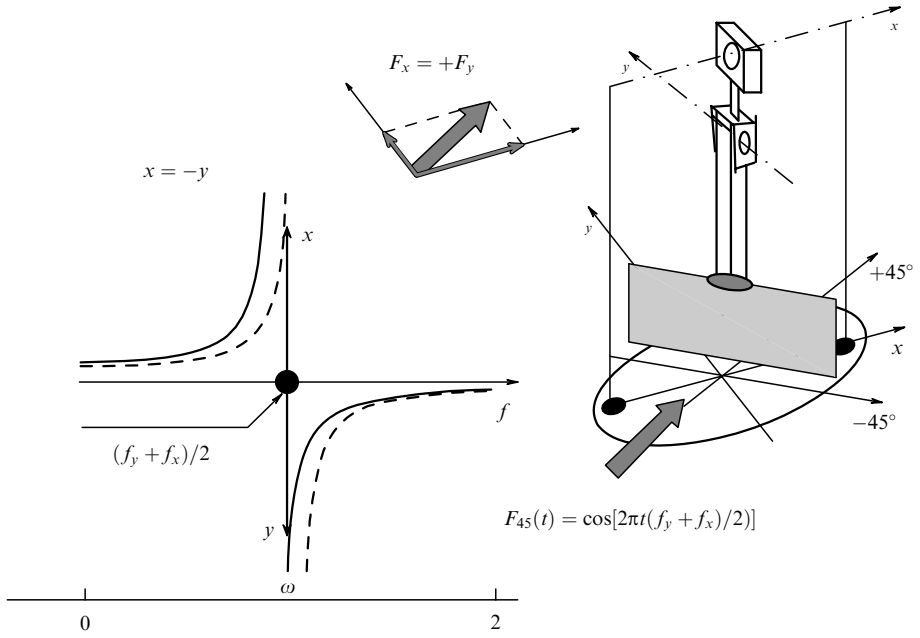

Figure 8. The design of a bi-frequency pendulum that uses, instead of threads, rigid aluminum elements and miniature ball bearings with minimum friction in them. This design prevents rotation of the pendulum around the vertical axis. A thin rigid sheet plays the role of a 'sail', providing strong aerodynamic friction, i.e., damping with respect to the motion perpendicular to the sail's plane. The particular choice of the sail's orientation was such that the motion in the $+45°$ direction was strongly dampened, while $-45°$ motion was supposed to induce almost no loss of mechanical energy. When the force at the mid-point frequency is applied in the $+45°$ direction, the steady-state response is generated in the $-45°$ direction. This results in almost zero loss of energy.

potential energy

$$0.5E_{ik}q_iq_k\,,$$

and dissipation function (half of the rate of energy dissipation, Joules per second)

$$0.5R_{ik}\,\frac{\mathrm{d}q_i}{\mathrm{d}t}\,\frac{\mathrm{d}q_k}{\mathrm{d}t}\,.$$

As usual, in all of these expressions summation over the repeating indexes is implied.

One can use the positive-definite quadratic form M_{ik} to define the scalar product in the linear space of generalized coordinates q_i. In other words, one can choose such combinations x_i of the original coordinates q_i, i.e., $x_i = \alpha_{ik}q_k$, that the mass matrix becomes the unit matrix in new coordinates x_i, and the linear space becomes Euclidean linear space with the scalar product x_jx_j. The next step is to use not just any combinations of new coordinates x_i, but to perform rotations in the above Euclidean real linear space. By definition, rotations preserve scalar product, i.e., the new mass matrix remains a unit matrix. Rotations in real Euclidean space allow diagonalization of any symmetric matrix. However, one can do this procedure with only one matrix at a time. If matrices E_{ik} and R_{ik} do not commute, one *cannot* reduce both of them to diagonal forms simultaneously.

This is exactly the physical situation with the mechanical device depicted in Fig. 8. Eigen-axes for the restoring force (for the potential energy matrix) are x and y. Meanwhile, eigen-axes for the friction force (for the dissipative function matrix) are $+45°$ and $-45°$. Diagonalization of these two matrices simultaneously via rotation of the coordinates x_i is impossible. One can formally define modes as such combinations of complex x- and y-amplitudes (or equivalently, as such combinations of $+45°$ and $-45°$ complex amplitudes), so that they evolve in time according to the exponential law, $\propto \exp(-\lambda^k t)$, $\lambda^k \equiv \mathrm{Re}(\lambda^k) + \mathrm{i}\,\mathrm{Im}(\lambda^k)$. These modes coincide neither with pure x and y motions, nor with pure $+45°$ and $-45°$ motions. Moreover, these modes are not orthogonal anymore. One cannot claim that total dissipated energy is the sum of squares of the amplitudes of each mode times dissipation rate $2\,\mathrm{Re}(\lambda^j) > 0$ for the corresponding mode. On the contrary, interference terms appear in the expression for the dissipation, and in some sense just those interference terms are responsible for the phenomenon of EIT.

6.2 Counterintuitive motion that models EIT

Suppose that the device above is subjected to a force at the 'carrier' frequency $f = (f_x + f_y)/2$, and that this force is applied in the $+45°$ direction (see Fig. 8) just as described in Section 5.2 The difference is that Section 5.2 dealt with a frictionless device.

Let us make an assumption, the validity of which will be confirmed by the results of subsequent calculations. Let us assume that this *strongly damped system* somehow *ignores damping completely*. Then one can use the counter-intuitive result from Section 5.1. Namely, steady-state motion will have a pure $-45°$ direction. But the motion in the $-45°$ direction does not result in any friction!

Two consequences follow from the above statement. First, one has justified the 'strange assumption'. Second, the force is applied in the direction of the strongest friction and the motion in this 'dissipative' direction is observed during the transient process. However, this system eventually comes to a counter-intuitive steady-state, in which dissipation is completely absent. Power transferred from the force to the device is zero, since the velocity vector is perpendicular to the force vector at all times. A very close analogy between this counter-intuitive behavior of our mechanical device and the EIT phenomenon exists; it will be discussed in Section 6.6.

Discussion of the mathematics and physics of the process should not detract the reader's attention from the most important pedagogical facts. First of all, the device which uses the screws with sharpened ends has actually been made by one of the authors in his garage out of easily available materials. Hence it may reasonably easily be made by students and teachers at the High-School level. Second, the device with all the electronics and computer support really and reproducibly demonstrated and continues to demonstrate the counter-intuitive features of motion described above.

6.3 Newton's Second Law for the system that models EIT

The equations describing Newton's Second Law for the above system are presented below. Cartesian axes x and y are assumed to be in the direction of the frame's plane and in the perpendicular direction, respectively. The choice of units allows the mass to be considered equal to 1. The motion of the pendulum in x and y directions is presented in the form

$$x(t) = 0.5\left[a_x(t)\exp\left(-\mathrm{i}\omega_0 t\right) + a_x^*(t)\exp\left(+\mathrm{i}\omega_0 t\right)\right], \quad (8)$$

$$y(t) = 0.5\left[a_y(t)\exp\left(-\mathrm{i}\omega_0 t\right) + a_y^*(t)\exp\left(+\mathrm{i}\omega_0 t\right)\right]. \quad (9)$$

Here, $\omega_0 = (\omega_x + \omega_y)/2 \equiv 2\pi(f_x + f_y)/2$ is the 'carrier' angular frequency, while the amplitudes $a_x(t)$, $a_y(t)$ and their complex conjugate values $a_x^*(t)$, $a_y^*(t)$ are supposed to be slowly varying functions of time. Introduce the notation $\Delta = (\omega_x - \omega_y)/2$ for half of the angular frequency difference between x- and y-eigenmodes. We will use the following method of 'deriving' the equations to the necessary degree of approximation. We suggest approximate equations to describe several limiting cases separately, and then we combine all the right-hand-side terms together.

If one ignores damping, here are the equations for slowly varying complex amplitudes $a_x(t)$, $a_y(t)$:

$$\frac{\mathrm{d}a_x(t)}{\mathrm{d}t} = -\mathrm{i}\Delta\, a_x(t), \qquad \frac{\mathrm{d}a_y(t)}{\mathrm{d}t} = +\mathrm{i}\Delta\, a_y(t). \quad (10)$$

Instead of deriving this approximate system of first-order differential equations, one can rely on the fact that equations (10) yield correct solutions in the absence of damping and of external forces:

$$a_x(t) = a_x(0)\exp\left(-\mathrm{i}\Delta t\right), \qquad a_y(t) = a_y(0)\exp\left(+\mathrm{i}\Delta t\right), \quad (11)$$

$$x(t) = \left|a_x(0)\right|\cos\left[\omega_x t - \psi_x\right], \qquad y(t) = \left|a_y(0)\right|\cos\left[\omega_y t - \psi_y\right]. \quad (12)$$

As for the damping, it was already assumed that strong friction takes place for the motion in the $+45°$-direction, with the amplitude damping constant Γ (s^{-1}), while the motion in the $-45°$-direction yields much weaker damping γ, i.e., $\gamma \ll \Gamma$. So, if one ignores x/y splitting of restoring forces but takes damping into account, these assumptions lead to the following equations and corresponding solutions:

$$a_{45}(t) = \frac{a_x(t) + a_y(t)}{\sqrt{2}}, \qquad a_{-45}(t) = \frac{a_x(t) - a_y(t)}{\sqrt{2}}, \quad (13)$$

$$\frac{\mathrm{d}a_{45}(t)}{\mathrm{d}t} = -\Gamma a_{45}(t), \qquad \frac{\mathrm{d}a_{-45}(t)}{\mathrm{d}t} = -\gamma a_{-45}(t), \quad (14)$$

$$a_{45}(t) = a_{45}(0)\exp\left(-\Gamma t\right), \qquad a_{-45}(t) = a_{-45}(0)\exp\left(-\gamma t\right). \quad (15)$$

The external force is represented in the form

$$\mathbf{F}_{\mathrm{real}}(t) = 0.5\left[\mathbf{F}(t)\exp\left(-\mathrm{i}\omega_0 t\right) + \mathbf{F}^*(t)\exp\left(+\mathrm{i}\omega_0 t\right)\right]. \quad (16)$$

Here, $\mathbf{F}(t) = \left\{F_x(t), F_y(t)\right\}$ is the slowly varying complex amplitude of the force. The system of Newton's Second Law equations for the motion of a frequency-degenerate frictionless pendulum under the influence of almost resonant force (16),

$$\frac{\mathrm{d}^2\mathbf{r}}{\mathrm{d}t^2} + \omega_0^2\mathbf{r} = \mathbf{F}_{\mathrm{real}}(t), \quad (17)$$

may be reduced to first-order equations for the slowly varying complex amplitudes:

$$\frac{\mathrm{d}\mathbf{a}}{\mathrm{d}t} \approx \mathbf{f}(t), \qquad \mathbf{f}(t) = \frac{\mathrm{i}\mathbf{F}(t)}{2\omega_0}. \quad (18)$$

Finally, derivation of the system of equations taking into account all these factors, angular frequency splitting Δ, damping Γ and γ, and the external force $\mathbf{F}$, is performed under the assumption that all these factors act *slowly*, i.e., have a relatively small instantaneous effect on the amplitudes, the effect being accumulated during many oscillations. Then one can simply add corresponding terms in the equations for the evolution of the slowly varying amplitude $\mathrm{d}\mathbf{a}/\mathrm{d}t$. For subsequent discussion, it is convenient to choose the equations in the $+45°/-45°$ axes:

$$\frac{\mathrm{d}a_{45}(t)}{\mathrm{d}t} + \Gamma a_{45}(t) + \mathrm{i}\Delta a_{-45}(t) = f_{45}(t), \qquad \frac{\mathrm{d}a_{-45}(t)}{\mathrm{d}t} + \gamma a_{-45}(t) + \mathrm{i}\Delta a_{45}(t) = f_{-45}(t). \quad (19)$$

If a monochromatic force is applied exactly at the 'carrier' frequency, then

$$f_{45}(t) = \mathrm{const}_1, \qquad f_{-45}(t) = \mathrm{const}_2,$$

and the steady-state solution is

$$a_{45} = \frac{1}{\Delta^2 + \Gamma\gamma}\left(\mathrm{i}\gamma f_{45} + \Delta f_{-45}\right), \qquad a_{-45} = \frac{1}{\Delta^2 + \Gamma\gamma}\left(\Delta f_{45} + \mathrm{i}\Gamma f_{-45}\right). \quad (20)$$

The most interesting result deals with the time-averaged power P dissipated by the pendulum:

$$P = 0.5\omega_0^2\left[\mathrm{i}\left(f_{45}a_{45}^* + f_{-45}a_{-45}^*\right)\right] + \mathrm{c.c.} \quad (21)$$

Substitution of the above solutions into the expression for P yields

$$P = \frac{m\omega_0^2}{\Delta^2 + \Gamma\gamma}\left(\gamma|f_{45}|^2 + \Gamma|f_{-45}|^2\right). \quad (22)$$

When the excitation occurs at the exact middle-point 'carrier' frequency [as was implied in Eqn (22)], one gets a very interesting result. Namely, the $+45°$-force results in dissipation proportional to the *small* friction constant

$\gamma \equiv \gamma_{-45}$, and vice versa, the force applied in the direction $-45°$ yields dissipation proportional to the *large* friction constant $\Gamma \equiv \Gamma_{45}$. It should be emphasized that, in a counter-intuitive manner, *low dissipation* appears when applying the force *in the direction of strong friction*. It is the statement about the unexpectedly small power dissipation that is so similar to the EIT phenomenon.

Equations (19) are simple enough, so that explicit analytical solutions may be found for any direction and frequency of the applied force: solutions that include both steady-state and transient processes. Comparison of analytical and numerical solutions of those equations may constitute a nice exercise for the students. Actually, the above SVEA equations for the complex amplitudes a_x, a_y are identical, up to the proper substitution of parameters, to the equations for a 3-level system's density matrix elements, if one limits oneself to the weak signal-field approximation.

6.4 Zero polarizability and vanishing scalar scattering of light

One can introduce the susceptibility tensor α_{ik} of the mechanical system depicted in Fig. 8, the ith component of vector **a** of the steady-state response to the kth component of the applied force vector **f**. The results of the demonstrations and calculations in Sections 5.1, 6.2, and 6.3 are counter-intuitive indeed. They may be described in the following terms. If $\gamma \equiv \gamma_{-45}$ is negligibly small, and if the force is applied at exactly the carrier frequency $\omega = \omega_0 = (\omega_x + \omega_y)/2$, then the component $\alpha_{+45,+45}$ of the susceptibility tensor α_{ik} is identically zero. This is easily interpreted. Indeed, force at the carrier frequency ω_0 is equidistantly below x-resonance and above y-resonance, so that positive and negative contributions by those resonances are cancelled identically (compare to Fig. 7). The component $\alpha_{+45,-45}$ of the susceptibility tensor is non-zero, but this component does not result in energy dissipation.

A similar situation may be found in resonant optics of alkali metals. Consider, for example, doublet resonance transition in sodium, Fig. 9. In the vicinity of resonance one can write the expression for the scalar part of polarizability in the form

$$\alpha(\omega) = \text{const} \cdot \left\{ \frac{f_{1/2}}{\omega_{1/2} - \omega} + \frac{f_{3/2}}{\omega_{3/2} - \omega} \right\}. \qquad (23)$$

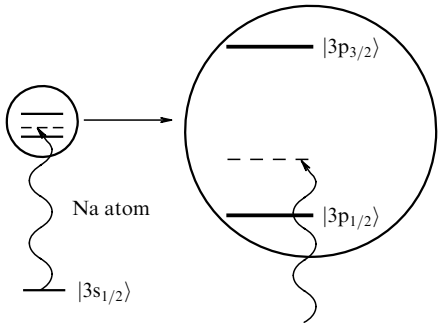

Figure 9. Illumination of a sodium (Na) atom by a resonant optical beam at the intermediate frequency point. The specific choice of that point $f = (2/3)f(s \to p_{1/2}) + (1/3)f(s \to p_{3/2})$ allows obtaining a zero scalar part of polarizability due to compensation of the contributions of the states $|3p_{1/2}\rangle$ and $|3p_{3/2}\rangle$. As a result, the scalar part of the resonant Rayleigh scattering is completely suppressed, and thus transparency of sodium vapor gas is increased [15].

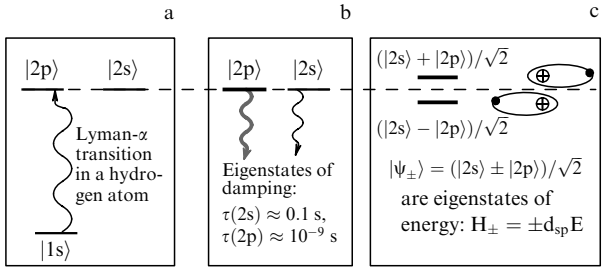

Figure 10. Electrostatically-induced transparency. (a) Resonant scattering (absorption) of Lyman-α light by a hydrogen atom in a weak external electrostatic field. (b) If the electrostatic field is ignored, then $|2s\rangle$ and $|2p\rangle$ are the eigenstates of the damping operator. (c) If damping is ignored, then the eigenstates of the Hamiltonian are $|\psi_+\rangle = |2p\rangle + |2s\rangle$ and $|\psi_-\rangle = |2p\rangle - |2s\rangle$ and the energy of the incident quanta is exactly at the mid-point between these two eigen-energies. As a result, polarizability is zero due to compensation of the contributions of the states $|\psi_+\rangle$ and $|\psi_-\rangle$, and the scattering/attenuation of light is suppressed completely: electrostatically-induced transparency.

Here, $f_{1/2} = 1/3$ and $f_{3/2} = 2/3$ are the oscillator strengths of the corresponding transitions $\{s \leftrightarrow p\}$. If the frequency ω is chosen between these transition lines, and ω is twice as close to the transition $\{s \leftrightarrow p(1/2)\}$ than to the transition $\{s \leftrightarrow p(3/2)\}$, then the scalar part of the polarizability is exactly zero. This nice and clear effect was predicted and observed experimentally about 3 decades ago [15]. The antisymmetric fluctuating part of polarizability still remains, since the ground state has spin 1/2; it leads to the antisymmetric scattering of light and, hence, to certain attenuation of the light beam.

6.5 Zero polarizability and electrostatically induced transparency

Consider Lyman-α transition in atomic hydrogen (Fig. 10a) and, for the purpose of the present section, let us ignore the electron's spin [16].

If one ignores the external electrostatic field (*ignores the linear Stark effect*), then $|2s\rangle$ and $|2p\rangle$ are the eigenstates of the damping operator (Fig. 10b). Indeed, the $|2s\rangle$-state is metastable with a very long lifetime, about 0.1 s. Meanwhile, the $|2p\rangle$-state exhibits strong damping due to spontaneous radiation at the transition $|2p\rangle \to |1s\rangle$, so that the lifetime is about 10^{-9} s.

On the contrary, *if one ignores damping*, but takes external electrostatic field into account, then the eigenstates of the Hamiltonian are $\big(|2s\rangle + |2p\rangle\big)/\sqrt{2}$ and $\big(|2s\rangle - |2p\rangle\big)/\sqrt{2}$, and the eigenvalues are symmetrically split by this linear Stark effect around the unperturbed energy of the originally degenerate pair of states $|2s\rangle$ and $|2p\rangle$.

The reader should be reminded: there is no orthogonal basis that allows one to diagonalize simultaneously both the damping operator and the Hamiltonian. This situation is very similar to the one considered in Section 6.1. Modal combinations that behave as $\exp(-\lambda^k t)$ do not coincide with any of the states mentioned above. Moreover, these modal combinations are both damped, $\mathrm{Re}(\lambda^k) > 0$, and they are non-orthogonal.

Just as in Section 6.2, let us assume that this *strongly damped system* somehow *ignores damping completely*. Then one can use the orthogonal Stark-split basis $\big(|2s\rangle + |2p\rangle\big)/\sqrt{2}$ and $\big(|2s\rangle - |2p\rangle\big)/\sqrt{2}$. In general, these states are not the 'modes' of the system. Since the weight of the dipole-active

$|2p\rangle$-state is the same in each of these states, the corresponding oscillator strengths are the same for the transitions from the $|1s\rangle$-state to each of the Stark states. If one tunes the frequency of incident light to the exact midpoint between the Stark-split transition frequencies, then polarizability becomes zero due to the exact compensation of the two contributions.

Zero polarizability has at least two important consequences. First, a zero induced dipole moment at the light frequency means that the Schrödinger's amplitude of the $|2p\rangle$-state *is not excited* in the steady state. This justifies the assumption about the possibility of ignoring the damping, since it was only the $|2p\rangle$-state that had anything to do with damping at all. Second, zero polarizability means the absence of absorption, i.e., it means transparency. *Quad erat demonstrandum*.

6.6 Electromagnetically induced transparency: spectral approach

The standard Λ-scheme of EIT is shown in Fig. 11 (see, e.g., [17, 18] and the details and references therein). Weak probe light is in resonance with strong dipole-active transition $|0\rangle \rightarrow |1\rangle$ and therefore is usually absorbed very strongly by the medium. A strong field of the so-called pump is applied to the medium; it is chosen to be in resonance with another strong transition, $|1\rangle \leftrightarrow |2\rangle$. The pump is not absorbed by the medium, since the states $|1\rangle$ and $|2\rangle$ are not originally populated. State $|0\rangle$ is stable in the absence of any fields, while state $|2\rangle$ is supposed to be metastable.

If one ignores damping, then the pump field leads to Rabi oscillations, so that the eigenstates of the Hamiltonian are $\big(|2\rangle + |1\rangle\big)/\sqrt{2}$ and $\big(|2\rangle - |1\rangle\big)/\sqrt{2}$. If the pump is in exact resonance with the transition frequency ω_{12}, then the eigenvalues of effective energy are split symmetrically around the original position of level $|1\rangle$. This the linear AC Stark effect, similar to the linear DC Stark effect.

If one ignores the AC Stark effect, then the eigenstates of the damping operator are $|1\rangle$ and $|2\rangle$, with strong damping in the $|1\rangle$-state and negligible damping in the $|2\rangle$-state. Actually, there is no orthogonal basis that allows the simultaneous diagonalization of both the damping operator and the Hamiltonian. Modal combinations that behave as $\exp(-\lambda^k t)$ do not coincide with any of the states mentioned above. Moreover, these modal combinations are both damped, $\mathrm{Re}\,(\lambda^k) > 0$, and they are non-orthogonal!

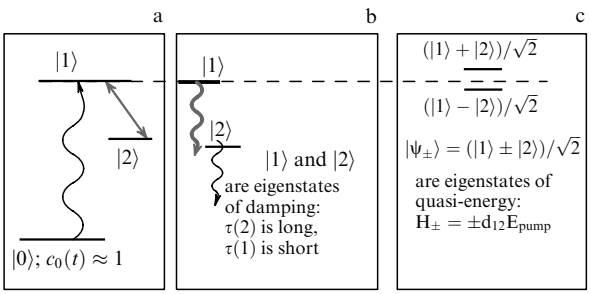

Figure 11. EIT: Electromagnetically induced transparency. (a) The so-called Λ-configuration for the observation of EIT. (b) If the external pump field at the frequency of the 1 – 2 transition is ignored, the eigenstates of the damping operator are $|1\rangle$ and $|2\rangle$. (c) If the damping of state $|1\rangle$ is ignored, then eigenstates of quasi-energy are $|\psi_+\rangle = |1\rangle + |2\rangle$ and $|\psi_-\rangle = |1\rangle - |2\rangle$, and the energy of the incident light quanta lies exactly at the mid-point between these two eigen-energies. As a result, polarizability is zero for the weak signal at the 0 – 1 transition due to the compensation of the two contributions from states $|\psi_+\rangle$ and $|\psi_-\rangle$. Resonant absorption of the signal at the 0 – 1 transition is thus suppressed by the presence of the pump at the 1 – 2 transition.

Just as in the above example, let us assume that this strongly damped system somehow ignores damping completely. Then one can use the Rabi-split basis $\big(|1\rangle + |2\rangle\big)/\sqrt{2}$ and $\big(|1\rangle - |2\rangle\big)/\sqrt{2}$. Since the weight of the dipole-active $|1\rangle$-state is the same in each of these states, the corresponding oscillator strengths are the same for the transitions from the $|0\rangle$-state to each of the Rabi states. If one tunes the frequency of incident light to the exact midpoint between the Rabi-split transition frequencies, then polarizability becomes zero due to the exact compensation of the two contributions.

Zero polarizability has at least two important consequences. First of all, a zero induced dipole moment at the frequency of the weak probe light means that the Schrodinger's amplitude of the $|1\rangle$-state *is not excited* in the steady-state regime. This justifies the assumption about the possibility of ignoring damping, since it was only the $|1\rangle$-state that had anything to do with damping at all. Second, zero polarizability means the absence of absorption, i.e., it means transparency.

6.7 Why now, and not in the 1920s?

Dr. H Schlossberg once asked us a pedagogically important question: "Why was such a simple and clear phenomenon (e.g., as in hydrogen) not discovered by the creators of quantum mechanics in the 1920s?" The answer may be divided into two parts related to two different limiting cases.

Case 1: splitting 2Δ of real parts of frequency eigenvalues is about 10 times larger than the linewidth Γ. Then, the suppression of the original absorption at the wavelength λ_0 of the 'old resonance' is not so surprising. A naive superposition would give a decrease in the absorption coefficient by the factor $4(\Gamma/\Delta)^2 = 1/25$. Modern refined theory predicts the decrease of absorption not to 4%, but down to exactly zero. Apparently, the creators of quantum mechanics had more important things to ponder in the 1920s than 4% corrections to intuitively clear predictions.

Case 2: splitting 2Δ of real parts of frequency eigenvalues is about 10 times smaller than the linewidth Γ. Here, the transition from absorption to transparency at the old resonant wavelength λ_0 is absolutely astonishing: a 100% drop in absorption, down to exact zero (if the coupled state was metastable). This should be compared to almost no change in absorption in the naive approach with a simple overlapping of two lines. So, why did the creators of quantum mechanics *not notice* such a large effect? Here is our (M J S and B Ya Z) hypothesis.

It was in the early 1900s when Michelson demonstrated experimentally that atomic spectral lines have finite width or structure. It was hard even to imagine[2] any experiments with spectral features narrower than radiative linewidths, which were still unresolved at the time. Meanwhile, the creators of quantum mechanics were very proud to understand and to explain to everybody the "Principle of Spectroscopic Stability": small perturbations do not change the integral of absorption coefficient β over the frequency. Indeed, a small spectral 'smear' of the new profile (which is the profile with a very narrow EIT-dip) kills this dramatic phenomenon. So, within the spectral accuracy available at the time, the creators

[2] Citing a Russian-language joke about a student: "The examiner asked me to describe a square trinomial, but I could not even imagine such a thing."

of quantum mechanics subconsciously felt right away that small splitting ($2\Delta \ll \Gamma$) does not matter much.

6.8 Carrier frequency and the envelope, x/y beats, and spin $1/2$ in quantum mechanics

One of the previous sections (4.6) was devoted to a demonstration showing an apparently surprising phenomenon: the envelope of the beats changes sign after one period of beats T_b and returns to the original value after $2T_b$ only. Several physical systems show analogous behavior.

The first example is the particle with spin $1/2$. Consider the quantum-mechanical wave function that corresponds to the z-projection m_z of the angular momentum. This wavefunction is transformed under the rotation by angle φ around the z-axis in a very simple way: it is multiplied by the factor $\exp(\mathrm{i}m_z\varphi)$. Since $m_z = +1/2$ or $m_z = -1/2$ for the spin-$1/2$ particle, rotation by $\varphi = 360^\circ$ yields the change of sign of the wave function; it is only after a 720° rotation that the wavefunction comes to its original value.

The second example deals with the so-called 2π-pulse, which may be considered 360° rotation around a certain coordinate axis in the equivalent spin space. The 2π-pulse, well-known in magnetic resonance and later in the optics of two-level systems, is described by the following solution of the Schrödinger equation for the amplitudes $c_1(t)$ and $c_2(t)$:

$$c_1(t) = \cos\frac{\varphi(t)}{2}\,, \qquad c_2(t) = \mathrm{i}\sin\frac{\varphi(t)}{2}\,,$$
$$\varphi(t) = \frac{d_{12}}{\hbar}\int_{-\infty}^{t} E(t')\,\mathrm{d}t'. \tag{24}$$

Elements of the density matrix, such as populations,

$$\rho_{11}(t) = \left|c_1(t)\right|^2, \qquad \rho_{22}(t) = \left|c_2(t)\right|^2,$$

and the polarization,

$$\rho_{21}(t) = c_2(t)c_1^*(t)$$

are restored after the action of a 2π-pulse, i.e., of a pulse with $\varphi(\infty) = 2\pi$. Meanwhile, the amplitudes themselves, $c_1(t)$ and $c_2(t)$, both change signs at $\varphi = 2\pi$; the sign is restored after two (2!) complete 2π-pulses only. This change of sign cannot be observed if one is really dealing with a two-level system. The presence of other levels, just like the presence of the reference pendulum in Section 4.6, allows one to get observable effects, including such an important effect as EIT.

6.9 Electromagnetically induced transparency: time-dependent approach

Consider again the simplest Λ-scheme of EIT, shown in Fig. 11. A strong auxiliary pump wave induces rapid Rabi oscillations with angular speed $\Omega_{12} = d_{12}E_{12}/\hbar$ between levels 1 and 2. However, those levels are originally empty and that is why the pump easily penetrates the medium at a large depth. The system originally occupies the ground state $|0\rangle$ only. A weak probe field is sent into the medium at the wavelength of the strong transition ω_{01} and, if the pump is absent, this transition results in the strong absorption of the field $E(\omega_{01})$.

If the probe field is switched 'on' stepwise at $t = 0$, and originally the amplitude $c_0(0) = 1$, then the amplitude $c_1(t)$ starts growing as $id_{01}E_{01}t/(2\hbar)$. It is this i-factor, which in the case without the pump would determine a positive imaginary part of the induced dipole and thus strong absorption at ω_{01}. However, this $\pi/2$-phased amplitude c_1, being exposed to pump E_{12}, *changes its sign* after one cycle of Rabi oscillations through level $|2\rangle$ (see Section 6.8 above). This means that absorption is changed into stimulated emission after one period of Rabi oscillations. The absorption is exactly balanced by emission after averaging over many Rabi cycles.

A particular demonstration of this idea with the use of the pendulum model from Section 6.1 may serve as an illustration of Ramsey's method of separated fields in magnetic resonance and atomic clocks. One starts with the pendulum at rest, and then switches 'on' the $+45^\circ$ force at the carrier frequency. It should be 'on' for a short pulse only, of the duration $\delta t \ll T_b$, and then turned 'off'. Then one watches for the pendulum to perform a complete period of beats $t = T_b$ and switches the same $+45^\circ$ carrier-frequency force 'on' for the same time duration δt. It is important that the signal-generator continues to generate a monochromatic 'carrier' signal with a stable phase; it is just needed that this signal has not been fed to the fans. This second short pulse of monochromatic force turns out to be in such a phase with respect to the oscillations that it results in almost a complete halt of the pendulum.

6.10 Wigner – von Neumann's theorem: level anti-crossing

Quantum-mechanical theorem about anti-crossing of the molecular terms with the same symmetry, by E Wigner and J von Neumann in 1929, may be illustrated via a bi-frequency pendulum on a rotary platform.

One should first use a mono-pivotal (and hence mono-frequency) pendulum, hanging at the center of a frame, and start the rotation of the platform. From the point of view of the rotating frame, each (of two) circularly polarized motion constitutes an eigenmode, as in Section 5.3. Co-rotation of the pendulum and the frame leads to a negative 'rotary Doppler effect': the frequency of rotation with respect to the frame is

$$\omega_{\mathrm{co}} = \omega_0 - \Omega\,,$$

where Ω is the angular velocity of the frame rotation. Counter-rotation yields a positive 'rotary Doppler effect':

$$\omega_{\mathrm{counter}} = \omega_0 + \Omega\,.$$

Consider now a bi-frequency pendulum, which has non-zero splitting of eigenfrequencies,

$$\omega_x - \omega_y = 2\Delta > 0\,,$$

i.e., $\omega_\pm = \omega_0 \pm \Delta$ at zero angular velocity of the platform, i.e., at $\Omega = 0$. However, if this pendulum is rotating fast, $\Omega \gg \Delta$, the situation must be almost the same as it was for the mono-frequency pendulum. The question is, will the two curves, which represent the dependence of eigenvalues on the angular velocity Ω, intersect? A theorem from quantum mechanics gives a hint: they will probably not cross each other.

Here, just as in Section 6.3, we will not derive the SVEA equations 'from first principles', i.e., from Newton's Second Law. Instead, we will 'guess' the appropriate right-hand-sides of these equations in such a manner that they yield correct solutions in the appropriate limiting cases.

We expect that a mono-pivotal pendulum, if considered in the rotating coordinate frame $\tilde{x}, \tilde{y}$, is described by the solutions:

$$\tilde{a}_x(t) = \tilde{a}_x(0)\cos(\Omega t) - \tilde{a}_y(0)\sin(\Omega t)\,,$$
$$\tilde{a}_y(t) = \tilde{a}_x(0)\sin(\Omega t) + \tilde{a}_y(0)\cos(\Omega t)\,.$$

The following elementary system of equations yields such a solution:

$$\frac{\mathrm{d}\tilde{a}_x}{\mathrm{d}t} = -\Omega\tilde{a}_y(t)\,, \qquad \frac{\mathrm{d}\tilde{a}_y}{\mathrm{d}t} = \Omega\tilde{a}_x(t)\,.$$

As a result, the system of equations for $\tilde{a}_x(t)$, $\tilde{a}_y(t)$ taking into account both splitting $2\Delta = \omega_x - \omega_y$ and rotation (the Coriolis force), becomes

$$\frac{\mathrm{d}\tilde{a}_x}{\mathrm{d}t} + \mathrm{i}\Delta\tilde{a}_x + \Omega\tilde{a}_y = 0\,,$$

$$\frac{\mathrm{d}\tilde{a}_y}{\mathrm{d}t} - \mathrm{i}\Delta\tilde{a}_y - \Omega\tilde{a}_x = 0\,.$$

Eigen-solutions of this system, i.e., solutions with the time-dependence $\exp(-\mathrm{i}\mu t)$, yield two eigenvalues, $\mu_{12} = \pm(\Delta^2 + \Omega^2)^{1/2}$. Keeping in mind the fact that the position vector $\tilde{\mathbf{r}}$ in the $(\tilde{x}, \tilde{y})$-plane is

$$\tilde{\mathbf{r}}(t) = 0.5\left[\tilde{\mathbf{a}}(t)\exp(-\mathrm{i}\omega_0 t) + \tilde{\mathbf{a}}^*(t)\exp(\mathrm{i}\omega_0 t)\right],$$

we come to two eigenfrequencies:

$$\omega = \omega_0 + (\Delta^2 + \Omega^2)^{1/2}\,, \qquad \omega = \omega_0 - (\Delta^2 + \Omega^2)^{1/2}\,. \quad (25)$$

The validity of this theorem is demonstrated with a pendulum by adiabatic transition from $\Omega = 0$ to $\Omega \gg \Delta$. The corresponding experiment is simple, but requires very smooth (very low) angular acceleration from $\Omega = 0$ to $\Omega \gg \Delta$. One can show in a simple experiment that, if started with the non-rotating low-frequency mode, the motion is adiabatically transformed into low-frequency circular motion, i.e., into co-rotation. And vice versa, the high-frequency linearly polarized mode is transformed adiabatically into a high-frequency circular motion, i.e., into counter-rotation. The possibility of predicting where the system will go is based on correct intuitive knowledge that the levels should not cross. This demonstration usually produces a very positive reaction among the audience at the high end of the education spectrum in quantum mechanics and mathematics.†

6.11 Nonlinear self-precession of an ellipse: quantitative consideration

Small deviations from equilibrium in the x- and y-directions are denoted as in Eqns (8), (9). We have derived the equation for a slowly varying envelope vector $\mathbf{a} = (a_x, a_y)$ accounting for nonlinearity in the first non-vanishing order of nonlinearity, i.e., in the 3rd order in the amplitude:

$$\frac{\mathrm{d}\mathbf{a}}{\mathrm{d}t} = -\mathrm{i}\omega_0\left(\frac{1}{8L^2}\right)(\mathbf{a}\cdot\mathbf{a}^*)\mathbf{a} + \mathrm{i}\omega_0\left(\frac{3}{16L^2}\right)(\mathbf{a}\cdot\mathbf{a})\mathbf{a}^* + O(a^4)\,. \quad (26)$$

There are many ways to get this SVEA equation. The method described below is typical for theoretical consideration of nonlinear optical phenomena. Namely, one can write this type of equation phenomenologically, with unknown coefficients, in the first non-vanishing order in amplitude (i.e., in cubic order), using time-shift invariance and axial symmetry:

$$\frac{\mathrm{d}\mathbf{a}}{\mathrm{d}t} = c_1(\mathbf{a}\cdot\mathbf{a}^*)\mathbf{a} + c_2(\mathbf{a}\cdot\mathbf{a})\mathbf{a}^*\,. \quad (27)$$

Consider now particular limiting cases.

1. Planar motion; e.g., $a_y(t) \equiv 0$, $a_x(t) \neq 0$. The problem of planar motion of a pendulum with an account for nonlinearity is well discussed in textbooks on classical mechanics (see, e.g., [19]). The maximum deflection angle $\varphi_{\max}$ (zero-to-top amplitude) is related to the complex amplitude a_x as

$$\varphi_{\max} = \arcsin\frac{|a_x|}{L} \approx \frac{|a_x|}{L}\,.$$

The equation of motion of a planar pendulum is

$$\ddot{\varphi} + \omega_0^2\sin\varphi = 0\,, \quad (28)$$

and, as is shown in numerous textbooks on mechanics, the frequency of weakly nonlinear oscillations decreases when the amplitude grows:

$$\omega = \omega_0\left[1 - \frac{\varphi_{\max}^2}{16} + O(\varphi_{\max}^4)\right] \approx \omega_0\left[1 - \frac{\mathbf{a}\cdot\mathbf{a}^*}{16L^2} + O(\varphi_{\max}^4)\right]. \quad (29)$$

It is worth noting that the use of slowly varying complex amplitudes from equations (8), (9) considerably simplifies the derivation of result (29) from equation (28) Here is this derivation. Taking the nonlinearity in its first non-vanishing approximation, one may reduce equation (28) to

$$\ddot{\varphi} + \omega_0^2\varphi \approx \frac{\omega_0^2\varphi^3}{3!}\,.$$

One can present the real function $\varphi(t)$ in the form

$$\varphi(t) = 0.5\left[\psi(t)\exp(-\mathrm{i}\omega_0 t) + \psi^*(t)\exp(\mathrm{i}\omega_0 t)\right],$$

where $\psi(t)$ is the slowly varying complex amplitude, $\varphi_{\max} = |\psi|$. Then, the SVEA equation for $\mathrm{d}\psi/\mathrm{d}t$ may be found, if one neglects the term $\mathrm{d}^2\psi/\mathrm{d}t^2$, so that

$$-2\mathrm{i}\omega_0\,\frac{\mathrm{d}\psi}{\mathrm{d}t} = \frac{\omega_0^2}{6}\,2\left\langle\varphi^3(t)\exp(\mathrm{i}\omega_0 t)\right\rangle_t,$$

where $\langle\ \rangle_t$ means averaging over many periods of $T_0 = 2\pi/\omega_0$. Substitution of the expression for φ via ψ and averaging yields

$$\frac{\mathrm{d}\psi}{\mathrm{d}t} = \frac{\mathrm{i}\omega_0|\psi|^2\psi}{16}\,.$$

2. Circular motion of a particle on a string in the presence of gravity is a problem from high-school physics. Conical

† The corresponding optical phenomenon, adiabatic transformation of linear (x or y) polarizations into circular (right or left) polarizations, may be and actually was observed with the use of an interesting medium consisting of gel with a large concentration of sugar. That created circular birefringence: right circularly polarized light had a lower phase velocity of propagation. The specimen was mechanically squeezed in such a way that deformation was zero at one end of the specimen and maximum at the other end. Strong deformation created linear birefringence: one of the linear polarizations (x-polarization to be exact) had lower phase velocity. When right circular polarization was sent to the specimen's non-deformed end, adiabatic transformation yielded linear x-polarization output at the strongly deformed end. Similar action took place for the transformation of left polarization into the y-linear one. Cells with deformed cholesteric liquid crystal are devices that potentially may use this optical phenomenon.

rotation of a pendulum with an angle $\varphi_{\max}$ measured from the vertical axis corresponds to

$$a_x = L\varphi_{\max}\,, \qquad a_y = \pm \mathrm{i} L\varphi_{\max}\,,$$

so that

$$\varphi_{\max}^2 = \frac{\mathbf{a}\cdot\mathbf{a}^*}{2L^2}\,, \qquad \mathbf{a}\cdot\mathbf{a} = 0\,.$$

The frequency of such rotation is

$$\omega_{\text{conical rotation}} = \omega_0(\cos\varphi_{\max})^{-1/2} \approx \omega_0\left(1+\frac{\varphi_{\max}^2}{4}\right) = \omega_0\left\{1+\frac{\mathbf{a}\cdot\mathbf{a}^*}{8L^2}\right\}, \tag{30}$$

so that $c_1 = -\mathrm{i}\omega_0/(8L^2)$. Combining this result with the result of equation (29), one comes to equation (26).

Let us return to the problem of self-precession of an elliptical orbit. If one denotes the maximum and minimum deflection angles from the vertical line for our almost elliptical motion by x_1/L and x_2/L, respectively, then the general solution to vector equation (26) is

$$\mathbf{a}(t) = \exp(\mathrm{i}\mu t)\left[x_1\mathbf{e}_1(t) + \mathrm{i}x_2\mathbf{e}_2(t)\right], \tag{31}$$

$$\mathbf{e}_1(t) = \mathbf{e}_x\cos(\Omega t) + \mathbf{e}_y\sin(\Omega t)\,, \qquad \mathbf{e}_2(t) = -\mathbf{e}_x\sin(\Omega t) + \mathbf{e}_y\cos(\Omega t)\,, \tag{32}$$

$$\mu = \frac{\omega_0}{16}\,\frac{x_1^2+x_2^2}{L^2}\,, \qquad \Omega \equiv \Omega_{\text{precession}} = \frac{3\omega_0}{8}\,\frac{x_1x_2}{L^2}\,. \tag{33}$$

The problem of a spherical pendulum has a well-known explicit analytical solution, which is found by taking into account conservation laws for energy and for the z-component of angular momentum. It should be noted, however, that it is impossible to reduce this problem to any equivalent problem of the motion of a particle in a weakly anharmonic field. The reason is that the kinetic energy term in the Lagrangian contains non-removable nonlinearity for the motion of a spherical pendulum. Apparently, that is why these simple expressions, Equations (31)–(33), which are valid with an accuracy on the order of $(x_1^2+x_2^2)/L^2$, are absent in published textbooks on classical mechanics (at least we could not find them there).

6.12 Second harmonic generation

The mechanical analog of this important optical process was also demonstrated with the use of the bi-frequency pendulum. First of all, one has to adjust quite precisely the ratio $\omega_x/\omega_y = 2$, i.e., $L_x/L_y = 1/4$, otherwise, weak nonlinear interaction will not be able to overcome even the small frequency mismatch $\delta = 2\omega_y - \omega_x$. The situation here is quite similar to the phase-matching problem in the crystals used in nonlinear optics.

Second, one must create the type of nonlinearity that would be non-symmetric with respect to $x \to -x$, $y \to -y$, similar to $\chi^{(2)}$-nonlinearity in optics; this nonlinearity requires the absence of the center of symmetry of the medium. The nonlinearity explored above in Sections 5.2 and 6.11 is analogous to $\chi^{(3)}$-nonlinearity in optics and therefore can not generate a second harmonic. The simplest way to arrange $\chi^{(2)}$-nonlinearity for the pendulum is to put a finger (or a pen or a knife) close to the vertical equilibrium position of the string. Then half of the cycle, the stage with $y > 0$, corresponds to the full length of the pendulum, while the other half of the cycle, the stage with $y < 0$, corresponds to a shorter length, the length from the finger to the bob. Unfortunately, while this arrangement produces the component of the force with a frequency $2\omega_y$, the projection of this force on the x-mode, $\omega_x = 2\omega_y$, is zero. This is similar to the search for the component of $\chi^{(2)}$, which is needed to provide for the interaction of the phase-matched o and e waves in optics. Therefore, we positioned two obstacles at opposite sides of the strings connecting the pivot to the central knot.

Here is what was observed. At a small amplitude of the fundamental-frequency mode (y mode), no energy transfer into the second harmonic mode (into the x mode) was visible during about 4 min of observation. At an amplitude around $y \approx 0.2L$ (φ_y about 0.2 rad) we observed quite a noticeable excitation of the second harmonic after about 30 s. The actual experiment was relatively difficult to set up and did not look very exciting, especially if the audience was uninitiated in optical second harmonic generation.

7. Conclusion

To conclude, the bi-frequency pendulum described above allows visualizing and better understanding numerous phenomena in physics and optics. It is a versatile educational tool: it allows teachers to provide something interesting, understandable, and emotionally gratifying for almost any point of the learning curve[3], from junior schoolchildren to research scientists. The authors have multiple years of experience in successfully using this device for teaching. A Microsoft Power Point presentation describing this device more in terms of pictures than in words and formulas can be downloaded from the URL http://admin.optics.ucf.edu/Soileau_Zeldovich_pendulum.ppt. Suggestions for further modifications and experiments are wholeheartedly welcomed.

Acknowledgments

A bi-frequency pendulum, tied to a pair of nails in the door frame, was part of teaching the kids in the family of the late Ya B Zeldovich, where in the 1950s one of the authors (B Ya Z) picked up the main idea. The same design of bi-frequency pendulum has been used (as became clear from subsequent discussions in the 1990s) at a number of universities in the USA, Israel, and, probably, in other countries. B Ya Z has garnered a number of ideas in optics, which later were illustrated with the use of the pendulum, from I I Sobelman and his colleagues V A Alekseev, A V Vinogradov, and T L Andreeva, as well as from S G Rautian. The idea to use a rotary platform came during the B Ya Z's work at the Joint Nonlinear Optics Laboratory of the Electrophysics Institute and the Chelyabinsk Polytechnic Institute in 1987–1994; B Ya Z is deeply grateful to G P Vyatkin, G A Mesyats, N D Kundikova, V A Krivoshchekov, Yu E Kapitskiĭ, and V P Beskachko for the creative atmosphere and concrete help. The authors express their gratitude for discussions of this teaching tool and technical help with the variants of the design to faculty and students of CREOL: College of Optics and Photonics of the University of Central Florida. Here are some of the names we would like to mention: M A Bolsh-

[3] Citation from a popular book of Soviet satire from the 1930s, *Golden Calf* by I Ilf and E Petrov: "'And what is the situation with the prostitution curve in your city?' Ostap asked with the sound of hope in his voice. 'It is going down decidedly', answered the uncooperative guide."

tyanskiĭ, P Copenhaver, O M Efimov, A A Goun, E Park, A Yu Savchenko, M G Moharam, and E W Van Stryland. The generous help of Barbara Abney in writing the text in English is very much appreciated.

8. Appendices

8.1 Appendix to Section 4.2: Lissajous figures and the Foucault pendulum

Senior participants in the demonstrations declare quite frequently that this is a *Foucault pendulum* and that the motion observed may be classified as *Lissajous figures*[4]. Teacher, beware: neither of the above statements is true. The Foucault pendulum was designed to demonstrate the Earth's rotation without watching the sun, moon, or stars. Being positioned at the Earth's North or South Pole, the Foucault pendulum must preserve the oscillation plane in the coordinate system of distant stars. Therefore, the oscillation plane will slowly rotate with respect to an observer on the Earth: one complete 360° turn in 24 h. Less trivial is the fact demonstrated by Foucault: a similar rotation at any other point on the Earth must also be observed, but with the perceived angular velocity diminished (multiplied) by factor $\sin\theta$, where θ is the latitude of the point; $\theta = +90°$ and $-90°$ at the North and South Poles, respectively[5]. From our point of view, this result is derived much more easily by decomposing the total vector of the Earth's angular velocity $\boldsymbol{\Omega} = \Omega_{\text{Earth}}\mathbf{e}_z$ into two components, the normal and the tangential to the local surface of the Earth:

$$\boldsymbol{\Omega} = \Omega_{\text{Earth}}(\mathbf{n}\sin\theta + \mathbf{t}\cos\theta)\,.$$

The next step is to declare that by symmetry and in the first-order approximation with respect to Ω only the normal component, $\Omega_{\text{Earth}}\sin\theta\,\mathbf{n}$, works, and then one reduces the problem to the evident case of the North Pole. The same logic lies behind the effect of Faraday rotation of polarization by a medium, when the external magnetic field vector **B** is tilted with respect to the propagation direction **n**. If one is interested in the linear effects with respect to **B**, only the longitudinal component $\mathbf{n}\,(\mathbf{B}\cdot\mathbf{n})$ works for Faraday rotation.

To function as a Foucault pendulum, a device must satisfy at least two conditions. First, once excited, free oscillations should not stop for at least a quarter of an hour, otherwise there will be nothing to observe. (Reminder: $\Omega_{\text{Earth}} = 15°/\text{h}$.) As a consequence, a typical Foucault pendulum is more than 10 m long and is usually very heavy (more than 50 kg). Second, the design must guarantee that the polarization plane would be preserved if the Earth were not rotating. Our pendulum satisfies neither of these requirements. First, the length and weight are limited in our case, and hence damping stops oscillations typically after several minutes. Second, by the very design, the oscillation plane for our pendulum periodically changes every half minute or so, without any influence from the rotation of the Earth or the platform.

Lissajous figures are 2D parametric-plot curves, for which x- and y-coordinates are oscillating as sinusoidal functions of *commensurate* frequencies. Our mechanical pendulum does not help in memorizing complicated trajectories. In this case, computer graphics or the use of an electronic oscilloscope is much more instructive.

8.2 Appendix to Section 4.2

Regarding the pendulum analogy with light propagation in uniaxial crystals, one should tilt the frame, so that the two ends of the thread are pivoted at different heights. Attentive consideration shows that a high frequency, f_x, is not changed at all (analog of an ordinary wave), while a low frequency, f_y, is diminished under such a tilt (analog of an extraordinary wave in a uniaxial crystal). Calculation of $f_y(\theta)$ is an interesting exercise for a classical mechanics course; we have not seen a corresponding solution in textbooks. Unfortunately, this analogy is superficial, since the underlying equations are dissimilar.

8.3 Appendix to Section 4.4: Adiabatic/non-adiabatic following

A very primitive example of the difference between fast (anti-adiabatic) and slow (adiabatic) processes uses the motion of a car under two different conditions. One is fast motion on ice, with a turn in the road denoted by shallow ruts. Inertia does not allow the car to turn, since the ice is slippery, and the car goes straight 'in absolute space', deviating from the curved road. In the other case, the car is in low-speed motion along a muddy road with very deep ruts. Here the car follows the curved road 'adiabatically' even if the driver tries to move straight. However, this analogy is also superficial, without similarity of the governing equations.

[4] According to legends, the late Academician Shalnikov used to say "Enough already. These are Lissajous figures," when pretending that something was beyond his understanding.

[5] Unfortunately, the derivation of this simple factor is obscured in most textbooks by excessive use of the vector product for the Coriolis force. Compare the citation from the book by V I Arnold, *Mathematical Methods of Classical Mechanics*, Springer-Verlag, p. 246: "In almost all textbooks, even the best, this (Maupertuis) principle is presented so that it is impossible to understand." (K Jacobi, Lectures on Dynamics, 1842–1843). V I Arnold continues: "I do not dare to break the tradition."

References

1. Landsberg G S *Optika* (Optics) 5th ed. (Moscow: Nauka, 1976)
2. Born M, Wolf E *Principles of Optics* 7th (expanded) ed. (Cambridge: Cambridge Univ. Press, 1999) [Translated into Russian (Moscow: Nauka, 1973)]
3. Akhmanov S A, Nikitin S Yu *Fizicheskaya Optika* (Physical Optics) (Moscow: Izd. MGU, 1998)
4. Vinogradova M B, Rudenko O V, Sukhorukov A P *Teoriya Voln* (Theory of Waves) 2nd ed. (Moscow: Nauka, 1990)
5. Sivukhin D V *Obshchiĭ Kurs Fiziki* Vol. 4 *Optika* (General Course of Physics. Optics) 2nd ed. (Moscow: Nauka, 1980)
6. Hecht E *Optics* 3rd ed. (Reading, Mass.: Addison-Wesley, 1998)
7. Landsberg G S *Elementarnyĭ Uchebnik Fiziki* (Elementary Textbook of Physics) Vol. III, 13th ed. (Moscow: Nauka, 2003)
8. Minnaert M G J *Light and Color in the Outdoors* (New York: Springer-Verlag, 1993) [Translated into Russian (Moscow: Nauka, 1969)]
9. Pikin S A, Blinov L M *Zhidkie Kristally* (Liquid Crystals) (Bibliotechka 'Kvant', Vyp. 20) (Library of "Quantum" Journal, Issue 20) (Moscow: Nauka, 1982)
10. Gorelik G S *Kolebaniya i Volny* (Oscillations and Waves) (Moscow: Fizmatgiz, 1959)
11. Zeldovich K B, software program 'freeware SQUARE PULSE', © K.B.Z., may be obtained for free from zeld@polly.phys.msu.ru
12. Blinov L M *Elektro- i Magnitooptika Zhidkikh Kristallov* (Electro- and Magnetooptics of Liquid Crystals) (Moscow: Nauka, 1978); Blinov L M, Chigrinov V G *Electrooptic Effects in Liquid Crystal Materials* (New York: Springer-Verlag, 1994)
13. Yeh P, Gu C *Optics of Liquid Crystal Displays* (New York: Wiley, 1999); Wu S-T, Yang D-K *Reflective Liquid Crystal Displays* (Chichester: Wiley, 2001)

14. Maker P D, Terhune R W, Savage C M *Phys. Rev. Lett.* **12** 507 (1964)
15. Tam A C, Au C K *Opt. Commun.* **19** 265 (1976)
16. Hakuta K, Marmet L, Stoicheff B P *Phys. Rev. Lett.* **66** 596 (1991)
17. Harris S E, Field J E, Imamoglu A *Phys. Rev. Lett.* **64** 1107 (1990)
18. Scully M O, Zubairy M S *Quantum Optics* (Cambridge: Cambridge Univ. Press, 1997) Ch. 7
19. Landau L D, Lifshitz E M *Mekhanika* (Mechanics) 5th ed. (Moscow: Nauka, 2004) [Translated into English (Oxford: Pergamon Press, 1976)]; Goldstein H *Classical Mechanics* 2nd ed. (Reading, Mass.: Addison-Wesley, 1980) [Translated into Russian (Moscow: Nauka, 1975)]